Chapter 5

Non–Adiabatic dynamics

In the previous chapter, we have analyzed the adiabatic limit of QD and QCMD for $\epsilon \to 0$. Both models have —under some non–crossing assumptions— the BO model as limit system. But, unfortunately, in real life applications non–adiabatic transitions of the quantum populations crucially influence the molecular dynamics. Therefore, a description of chemical reactions based on an adiabatic limit model yields essentially wrong results. Thus, the correct computation of non–adiabatic deviations from adiabatic motion is a major goal in the construction of new reduced models to QD.

Non–adiabatic effects can be interpreted as *resonance effects* between the classical and quantum subsystems. They take place whenever the *spectral gap* between the energy levels of the quantal subsystems become small enough in comparison to ϵ.

In many examples, the dynamics happens to be only "mildly" non–adiabatic. That means that they can be described by decisive but "small" corrections to the adiabatic evolution. Therefore, those applications seem to be best prepared for models which include some relevant higher order terms in ϵ. A first approach [122] to such a model was presented by Zener in the 30's. The Landau–Zener formula allows to compute the asymptotic effects of avoided crossings in various specific situations [70, 122, 109]. The higher order expansion terms of QCMD are presented in Sec. §3.1.

Since the theoretical description of the first expansion terms of the solution does not suffice for realistic application problems, numerous algorithm–oriented methods have been proposed to include non–adiabatic effects. The most prominent embody surface hopping methods [117, 115, 51, 5], mean-field models like QCMD and TDSCF [36, 15, 16, 104], path integral oriented methods [18, 92, 85], or the semi-classical initial value representation [82, 83]. A surface–hopping method [104] which is based on QCMD is introduced in §4. Unfortunately, all these algorithmic models are only heuristically justified. A rigorous mathematical derivation from QD has still not been given for any of these models. Thus, it seems obvious that for each of these models there are pros and cons in application to realistic applications.

Recently, a novel approach to an mathematically justifiable model was presented by Martens and others [75, 61]. Based on a density matrix description for the coupling between quantum and classical subsystem they introduced the so-called *quantum-classical Liouville equation (QCL)*. In [103] Schütte gives a rigorous analysis of the approximation properties and proposes a method to solve the arising equations. This method might be a pattern for the construction of either deterministic [28] or stochastic [61] schemes. Sec. §5 gives a short overview over the basic ideas which lead to QCL.

§1 Non–Adiabaticity in QD

In order to keep the notation as simple as possible, we will discuss the case of a full quantum system which is already discretized with respect to x. Thus, let

us discuss the time–dependent Schrödinger equation

$$i\epsilon\,\partial_t\Psi_\epsilon \;=\; \left(-\frac{\epsilon^2}{2}\Delta_q \;+\; H(q)\right)\;\Psi_\epsilon \tag{5.1}$$

where $H(q) = \big(V_{\lambda\mu}(q)\big)$ is a family of complex Hermitian $N\times N$ matrices, $q\in\mathbb{R}^d$ and $\Psi_\epsilon : \mathbb{R}^d\times\mathbb{R}\to\mathbb{C}^N$ the vector valued solution. The initial value is given by $\Psi_* = \Psi_\epsilon(\cdot, t=t_0)$. Furthermore, let for $H(q)$ apply:

(A1') the q–parameterized Hamiltonian $H(q)$ is smoothly diagonalizable

$$H(q)e_\lambda(q) = E_\lambda(q)e_\lambda(q) \tag{5.2}$$

(E4) and exclude energy level crossings

$$E_\lambda(q) = E_\mu(q) \quad \text{for} \quad \lambda\neq\mu. \tag{5.3}$$

Now, expand the solution $\Psi_\epsilon = \Psi_\epsilon(q,t)$ of (5.1) in the adiabatic basis e_λ:

$$\Psi_\epsilon(q,t) \;=\; \sum_{\lambda=1}^{N} c_\epsilon^\lambda(q,t)\; e_\lambda(q). \tag{5.4}$$

and obtain via (5.1) the equation of motion for the expansion coefficients $c_\epsilon = (c_\epsilon^\lambda(q,t))$

$$i\epsilon\,\partial_t c_\epsilon = E\,c_\epsilon \;-\; \frac{\epsilon^2}{2}\Delta_q\,c_\epsilon + \frac{\epsilon^2}{2}T\,c_\epsilon \;-\; \epsilon^2\,\mathcal{C}\cdot D_q\,c_\epsilon, \tag{5.5}$$

with initial values $c_* = (c_\epsilon^\lambda(q,t_0))$. The matrix-valued functions E, T and the tensor-valued function $\mathcal{C}$ (the *coupling tensor*) are given by

$$\begin{array}{lllll} E = E(q) = \mathrm{diag}(E_\lambda(q)) & & & & \\ T = T(q) = (T_{\lambda\mu}(q)) & & T_{\lambda\mu} &=& \langle e_\lambda(q)|\Delta_q e_\mu(q)\rangle \\ \mathcal{C} = \mathcal{C}(q) = (d^j_{\lambda\mu}(q)) & & d^j_{\lambda\mu} &=& \langle e_\lambda(q)|D_{q_j} e_\mu(q)\rangle \\ \text{with} & (\mathcal{C}\cdot D_q c_\epsilon)_\lambda &=& \sum_{j,\mu} d^j_{\lambda\mu}\,D_{q_j}\,c_\epsilon^\lambda, \end{array} \tag{5.6}$$

where $\langle\cdot|\cdot\rangle$ denotes the scalar product in $L^2(\mathbb{R}^d)^N$.

The first two terms on the RHS describe the adiabatic evolution on the energy levels given by E_λ, whereas the remaining two terms represent the non–adiabatic coupling of the motion on these levels.

§2 An Avoided Crossing Example

In the subsequent, let us consider the particularly simple test case where the quantum subsystem can be described as a two state system and the classical subsystem is one-dimensional. Thus, $q:\mathbb{R}\to\mathbb{R}^1$ and the full Schrödinger equation has the form:

$$i\epsilon\,\partial_t\Psi_\epsilon \;=\; \left(-\tfrac{\epsilon^2}{2}\mathcal{T}_q \;+\; H(q)\right)\;\Psi_\epsilon, \tag{5.7}$$

with $H(q)$ and $\mathcal{T}_q$ denoting 2×2 Hermitian matrices:

$$\mathcal{T}_q = \begin{pmatrix} \Delta_q & 0 \\ 0 & \Delta_q \end{pmatrix} \quad \text{and} \quad H(q) = \begin{pmatrix} V_{11}(q) & c \\ c & V_{22}(q) \end{pmatrix}.$$

The wave function $\Psi_\epsilon \in (L^2(\mathbb{R}))^2$ consists of two components $\Psi_\epsilon = (\Psi_\epsilon^1, \Psi_\epsilon^2)^T$, each of which a function in q and t.

Herein, we choose the potentials to be $V_{11}(q) = q^2$ and $V_{22}(q) = 1/q$. The interpretation is the following: V_{11} describes a harmonic bond, V_{22} a repulsive potential, and $V_{12} = V_{21} = c$ a weak coupling between these two (electronic) configurations. We choose $\epsilon = 0.01$ which is a suitable scaling for electrons. In the following we set $c = 0.1$. For the choices made, Fig. 5.1 shows the energy eigenvalues $E_1 = E_1(q)$ and $E_2 = E_2(q) < E_1(q)$ of $H(q)$ and the corresponding off-diagonal entry of the non–adiabatic coupling matrix d_{12}. Notice that there

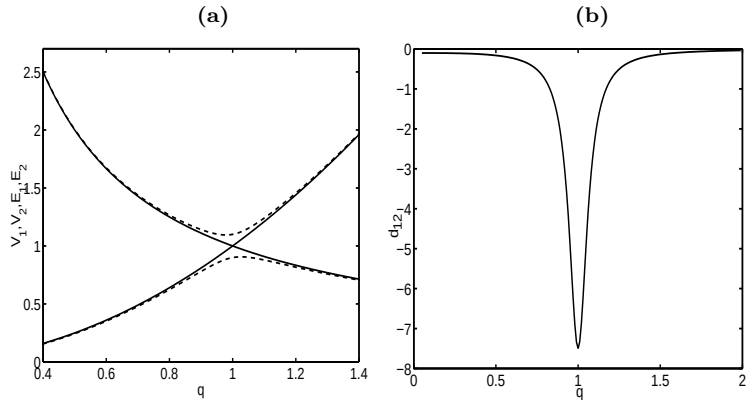

Figure 5.1. **(a)** Potentials V_{11} and V_{22} (*solid lines*) and energy levels E_1 and E_2 (*dashed lines*) versus q. **(b)** Non–Adiabatic coupling matrix element d_{12} versus q

is some "transition zone" around $q = 1$ where the gap between the two energy levels is minimal and the coupling matrix entry significantly large.

We are interested in the following initial condition: Let $e_1 = e_1(q)$ be the eigenvector to E_1, $q_0 = 0.4$ and $p_0 = 1$. Then the initial wave function is centered at q_0 with momentum expectation p_0 and the energy level E_1 is occupied only, i.e.,

$$\Psi(q, t = 0) \;=\; \tfrac{1}{A} \exp\left(-\tfrac{1}{4\epsilon}(q - q_0)^2 \;-\; \tfrac{i}{\epsilon} p_0 q\right) \cdot e_1(q_0).$$

Figure 5.2 illustrates the true quantum dynamical solution of (5.7) for the initial condition given. We observe that the centers of the two components Ψ_ϵ^1 and Ψ_ϵ^2 of the wave function diverge when crossing the transition zone. The motion of each of these two centers is governed by the Born-Oppenheimer solutions on the corresponding[1] energy levels E_1 and E_2 (cf., Fig. 5.3 (**b**)). We can conclude that the non–adiabatic effect of the transition zone induces some significant population of the initially unoccupied energy level whereas the motion outside of the transition zone is governed by classical dynamics on the energy levels

[1] Away from the transition zone, the eigenvectors of H are approximately given by the two unit vectors.

and induces the observed divergence. Obviously, a *single* QCMD trajectory – even when representing the correct population dynamics – cannot reproduce this divergence. Thus, later on we follow the idea of splitting QCMD trajectories leading to a specific variant of so-called surface hopping.

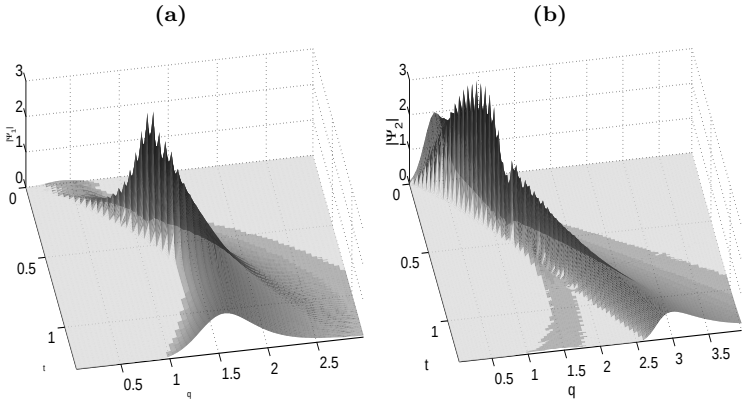

Figure 5.2. Avoided Crossing Example: Evolution of the full QD wave packet in q and t for parameter $\epsilon = 0.01$. Absolute value of **(a)** Ψ^1_ϵ and **(b)** Ψ^2_ϵ

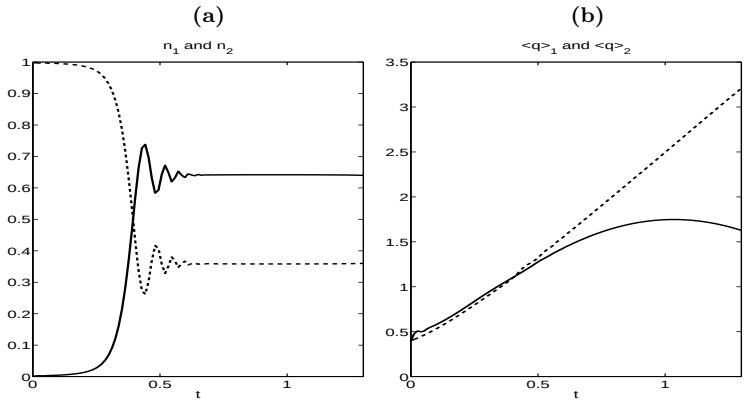

Figure 5.3. Full QD for $\epsilon = 0.01$: **(a)** Statistical weights $n_1 = \|\Psi^1_\epsilon\|_2^2$ and $n_2 = \|\Psi^2_\epsilon\|_2^2$ of the two components versus t. **(b)** Position expectation values $\langle q\rangle_\lambda = \langle \Psi^\lambda_\epsilon, q\Psi^\lambda_\epsilon\rangle / n_k$ of the components

§3 Non–Adiabaticity in QCMD

One can easily inspect the deviation of QCMD from its adiabatic limit if we reformulate its equation of motion (2.9) in the coordinate system given by the eigenstates of the Hamiltonian $H(q) \in \mathbb{C}^{N\times N}$. In terms of the notation introduced above, we therefore make the following ansatz for the QCMD-wave packet ψ_ϵ:

$$\psi_\epsilon(t) \;=\; \sum_\lambda c^\lambda_\epsilon(t)\, e_\lambda(q_\epsilon(t)).$$

Inserting this into the QCMD equations we find

$$\begin{aligned} i\epsilon\partial_t c_\epsilon^\lambda &= E_\lambda(q_\epsilon)c_\epsilon^\lambda - i\epsilon\dot{q}_\epsilon \sum_\mu d_{\lambda\mu}(q_\epsilon)\, c_\epsilon^\mu, \\ \ddot{q}_\epsilon &= -\nabla_q \sum_\lambda |c_\epsilon^\lambda|^2\, E_\lambda(q_\epsilon) - \sum_{\lambda\mu}(c_\epsilon^\lambda)^* c_\epsilon^\mu\, \Delta E_{\lambda\mu}(q_\epsilon)\, d_{\lambda\mu}(q_\epsilon), \end{aligned} \tag{5.8}$$

with coupling matrix elements $d_{\lambda\mu} = (d^j_{\lambda\mu})$ and energy gaps $\Delta E_{\lambda\mu}(q) = E_\lambda(q) - E_\mu(q)$. Thus, the non–adiabatic coupling between the energy levels in QCMD is governed by the coupling matrix $(d_{\lambda\mu})$. Whenever Assumption (E4) from above is valid one can show [13] that the deviation from the adiabatic solution induced by this non–adiabatic coupling is of order $\mathcal{O}(\epsilon)$!

§3.1 First order corrections

Additionally, we are able to construct explicit expressions for the first order deviation terms: To this end, the coefficients c_ϵ^λ must be represented in polar coordinates, i.e.,

$$c_\epsilon^\lambda(t) = \sqrt{\theta_\epsilon^\lambda(t)}\, \exp\left(-\frac{i}{\epsilon}\varphi_\epsilon^\lambda(t)\right),$$

with initial values

$$c_*^\lambda = \sqrt{\theta_*^\lambda}\, \exp\left(-\frac{i}{\epsilon}\varphi_*^\lambda\right),$$

and one introduces the Born–Oppenheimer angle $\varphi^\lambda_{\rm BO}$ as the solution of

$$\dot{\varphi}^\lambda_{\rm BO} = E_\lambda(q_{\rm BO})$$

along the BO solution $q_{\rm BO}$ with $\varphi^\lambda_{\rm BO}(0) = \varphi_*^\lambda$. In addition, we have to exclude all symmetric resonances of order four:

(E5) let in some neighborhood of $q_{\rm BO} = q_{\rm BO}(t)$ hold

$$E_\lambda(q) + E_\mu(q) \neq E_\eta(q) + E_\xi(q) \quad \text{for} \quad \lambda \neq \eta,\, \lambda \neq \xi,\, \mu \neq \eta,\, \mu \neq \xi. \tag{5.9}$$

This condition allows to compute the non–adiabatic corrections to the adiabatic limit up to the leading orders in ϵ [13, 86]:

$$\begin{aligned} q_\epsilon &= q_{\rm BO} + \epsilon^2\delta q_{2,\epsilon} + \mathcal{O}(\epsilon^3), & \dot{q}_\epsilon &= \dot{q}_{\rm BO} + \epsilon\,\delta\dot{q}_{1,\epsilon} + \mathcal{O}(\epsilon^2), \\ \theta_\epsilon^\lambda &= \theta_*^\lambda + \epsilon\,\delta\theta^\lambda_{1,\epsilon} + \epsilon^2\delta\theta^\lambda_{2,\epsilon} + \mathcal{O}(\epsilon^3), & \varphi_\epsilon^\lambda &= \varphi^\lambda_{\rm BO} + \mathcal{O}(\epsilon^2). \end{aligned}$$

since $\theta^\lambda_{\rm BO} = \theta_*^\lambda$. Under the assumption (E5), we have the following two theorems:

Theorem 5.1 (Appendix C of [13]) *The first order corrections are given by*

$$\begin{aligned} \delta\theta^\lambda_{1,\epsilon} &= 2\left(\Theta^\lambda_{1,0} - \sum_{\mu\neq\lambda,j} \frac{\dot{q}^j_{\rm BO}\sqrt{\theta_*^\lambda\theta_*^\mu}}{\Delta E_{\lambda\mu}(q_{\rm BO})} \sin\left(\epsilon^{-1}\left(\varphi^\lambda_{\rm BO} - \varphi^\mu_{\rm BO}\right)\right) d^j_{\lambda\mu}(q_{\rm BO})\right) \\ \Theta^\lambda_{1,0} &= \sum_{\mu\neq\lambda,j} \frac{\dot{q}^j_\epsilon(0)\sqrt{\theta_*^\lambda\theta_*^\mu}}{\Delta E_{\lambda\mu}(q_\epsilon(0))} \sin\left(\epsilon^{-1}\left(\varphi_*^\lambda - \varphi_*^\mu\right)\right) d^j_{\lambda\mu}(q_\epsilon(0)) \\ \delta\dot{q}^\lambda_{1,\epsilon} &= \sum_{\lambda,\mu} \sqrt{\theta_*^\lambda\theta_*^\mu}\sin\left(\epsilon^{-1}\left(\varphi^\lambda_{\rm BO} - \varphi^\mu_{\rm BO}\right)\right)\, d^j_{\lambda\mu}(q_{\rm BO}). \end{aligned}$$

This result implies $c_\epsilon^\lambda(t) = \sqrt{\theta_*^\lambda}\,\exp(-\frac{i}{\epsilon}\varphi_{\mathrm{BO}}^\lambda(t)) + \mathcal{O}(\epsilon)$.

§3.2 Second order corrections of the populations

Moreover, in the particular case, that initially the wave packet occupies only one of the eigenstates, say e_μ, Thm. 5.1 states that the first order corrections vanish identically. Then, the following is valid for the second order corrections:

Theorem 5.2 (Thm. 1 of [86]) *Whenever $\theta_*^\lambda = \delta_{\mu,\lambda}$, the first order corrections for the populations in state λ, $\lambda \neq \mu$, vanish, $\delta\theta_{1,\epsilon}^\lambda = 0$, and the second order corrections are given by*

$$\begin{aligned}\delta\theta_{2,\epsilon}^\lambda(t) \;=\; &\left(\frac{B_{\mathrm{BO}}^{\lambda\mu}(t)}{\Delta E_{\lambda\mu}^{\mathrm{BO}}(t)}\right)^2 + \left(\frac{B_{\mathrm{BO}}^{\lambda\mu}(0)}{\Delta E_{\lambda\mu}^{\mathrm{BO}}(0)}\right)^2 \\ &- 2\,\frac{B_{\mathrm{BO}}^{\lambda\mu}(t)}{\Delta E_{\lambda\mu}^{\mathrm{BO}}(t)}\frac{B_{\lambda\mu}^{\mathrm{BO}}(0)}{\Delta E_{\lambda\mu}^{\mathrm{BO}}(0)}\cos\left(\frac{\varphi_{\mathrm{BO}}^\lambda(t) - \varphi_{\mathrm{BO}}^\mu(t)}{\epsilon}\right) + \mathcal{O}(\epsilon)\end{aligned} \tag{5.10}$$

with $B_{\mathrm{BO}}^{\lambda\mu} := -\langle e_\lambda(q_{\mathrm{BO}}), D_{q_j} e_\mu(q_{\mathrm{BO}})\rangle \cdot \dot{q}_{\mathrm{BO}}$ and $\Delta E_{\lambda\mu}^{\mathrm{BO}} = \Delta E_{\lambda\mu}(q_{\mathrm{BO}})$.

§3.3 Numerical example

For the avoided crossing example of §2, we have computed the QCMD as well as the Born–Oppenheimer dynamics. Based on the BO motion, we have calculated the second order correction terms (5.10) of the population of the initially unoccupied state θ_ϵ^2. A comparison between this analytically obtained excitation dynamics and the QCMD population θ_ϵ^2 of the simulation is given in Fig. 5.4 **(a)** and **(b)** for different time spans.

Obviously, the approximation is just valid in a region, where the QCMD motion is close to the corresponding BO motion. Thus, the second order ap-

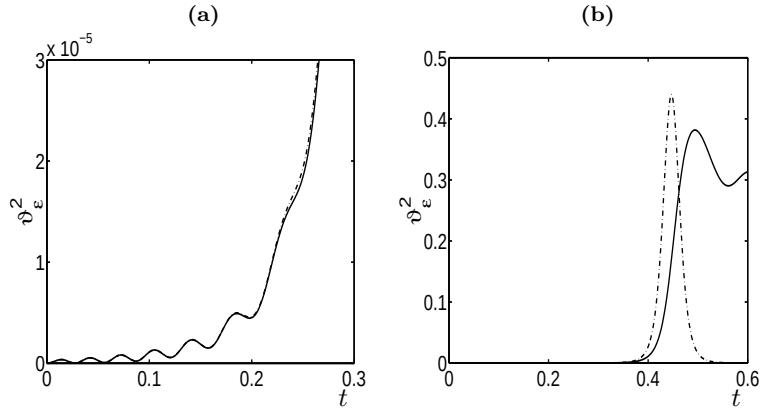

Figure 5.4. Population of initially unoccupied state θ_ϵ^2 versus time t for different time spans. Population θ_ϵ^2 computed in a QCMD simulation (*solid lines*) and via the second order approximation presented in Thm. 5.2 (*dashed dotted lines*)

proximation based on the expansion around the Born-Oppenheimer solution fails in the transition zone. Nonetheless, the initial excitation of the second

level is correctly represented. This might help as an indicator of a beginning excitation of a previously unoccupied energy level as, for example, in the QCMD surface hopping algorithm presented in the following section.

§4 QCMD-based Surface Hopping

Due to the previous sections, a single QCMD trajectory may reproduce the QD evolution if ϵ is small enough, resonances (level crossings) are avoided, and the initial QD wave packet $\Psi(\cdot, t = t_0)$ is an approximate δ-function in the q-direction (cf., eqs. (2.2) and (3.11)). Nevertheless, we have seen in Sec. §2 that a single classical trajectory cannot reproduce a divergent dynamics in the case of non–adiabatic population redistributions. Since the full Schrödinger equation is linear, we may decompose the actual $\Psi(\cdot, t = t_0)$ into finitely many approximate δ-functions at appropriately distributed locations q_*^j and momenta $\dot{q}_*^j$. Thus, we might simulate a *QCMD trajectory bundle* starting at all the different $(q_*^j, \dot{q}_*^j)$ each with an initial x-wave function $\psi_*^j = \Psi(q_*^j, t = t_*)$. In a simulation of this kind, every QCMD-trajectory exhibits its own non–adiabaticity, but any non–adiabatic effect mediated by coupling between different trajectories is excluded.

In [116], the "father" of the so-called *surface hopping* techniques [117, 114], C.J. Tully, interprets the non–adiabatic effects in full QD as a composition of two different contributions: the non–adiabatic effects along each QCMD trajectory given by the solution of (5.8) and the contribution of the coupling between the trajectories in the QCMD particle bundle constructed to represent the QD wave function.

In this section, a surface hopping algorithm is introduced which makes use of the QCMD solution in order to include non–adiabatic effects. However, the reader should notice that this algorithm is just a heuristic concept only justified by numerical experiment. There is no rigorous mathematical evidence on the approximation properties with respect to the full quantum dynamics.

§4.1 Surface Hopping Algorithm

Suppose that we start a trajectory at position q_* with initial momentum $\dot{q}_*$ on the μth energy surface E_μ, i.e., with initial QCMD-wave function $\psi_* = e_\mu(q_*)$. In the following we denote the QCMD trajectory, i.e., the solution of (2.9), by $(q(t + t_0), \dot{q}(t + t_0), \psi(t + t_0)) = \mathrm{QCMD}(t|\, q(t_0), \dot{q}(t_0), \psi(t_0))$, omitting the ϵ-dependence since ϵ now is assumed to have a fixed value. The key assumption of surface hopping techniques is as follows: We can use the non–adiabatic effects along the QCMD trajectory as an indicator for the deviation of the full QD evolution from its adiabatic limit. In other words: Whenever the non–adiabatic effects along the QCMD trajectory induce populations on some level $\lambda \neq \mu$ which are significantly larger than zero, i.e., whenever $\theta_\lambda \geq tol > 0$, one should additionally follow the path which corresponds to the dynamics on level E_λ. But instead of starting a new trajectory on this level in every such case which would finally yield a combinatorial explosion, one stochastically decides whether or not to switch the energy level ("make a hop or not"). This algorithm should be constructed so that, at any instance in time for a large ensemble of particles,

the fraction of trajectories assigned to any energy surface is approximately equal to the relative population of this energy level.

This idea leads to the following *QCMD-based surface hopping variant* of Tully's surface hopping algorithm:

1. Start with a large ensemble of N independent QCMD-trajectories with states $(q_*^j, \dot{q}_*^j, \psi_*^j)$, $j = 1, \dots, N$, where every ψ_*^j belongs to a certain energy level μ_j, that is, satisfies $\psi_*^j = e_{\mu_j}(q_*^j)$. This trajectory bundle has to represent the initial QD wave packet $\Psi(\cdot, t = t_*)$ in the ensemble sense.

2. For every single trajectory $j = 1, \dots, N$ repeat the following propagation:

   (a) Propagate the trajectory along the QCMD solution

   $$(q_{m+1}^j, \dot{q}_{m+1}^j, \psi_{m+1}^j) \;=\; \mathrm{QCMD}(\Delta t \,|\, q_m^j, \dot{q}_m^j, \psi_m^j)$$

   for some large time span Δt.

   (b) Compute the transition zone indicator Ξ for the trajectory on level μ_j:

   $$\Xi \;=\; \sum\nolimits_{\lambda \neq \mu_j} \left| \frac{\langle e_\lambda(q_{m+1}^j), \nabla_q e_{\mu_j}(q_{m+1}^j) \rangle \;\dot{q}_{m+1}^j}{\Delta E_{\lambda\mu_j}(q_{m+1}^j)} \right|$$

   (c) If the indicator Ξ exceeds a preset threshold value Ξ_*, decide whether to make a hop or not (Step 2d). Otherwise continue with the propagation (Step 2a).

   (d) Compute the level populations $\theta_\lambda = |c_\lambda^j|^2$ with $c_\lambda^j = \langle e_\lambda(q_{m+1}^j), \psi_{m+1}^j \rangle$. In the last step the trajectory j started on the energy level E_{μ_j}; the energy level for the next step is selected via the hopping probabilities $P(\mu_j \to \lambda) = |c_\lambda^j|^2$, $\mu = 1, \dots, n$. If due to this random decision a hop onto the lth level is carried out, then set the wave function on energy level E_λ and accordingly modify the momentum:

   $$\psi_{m+1}^j = e_\lambda(q_{m+1}^j), \quad \dot{q}_{m+1}^j = \mu(\mu_j \to \lambda, q_{m+1}^j, \dot{q}_{m+1}^j), \;\text{ and }\; \mu_j = \lambda$$

   Otherwise – if the random decision is to stay on level μ_j – do nothing.

   (e) Continue the propagation with Step 2a.

The reader might have noticed that the transition zone indicator Ξ is deduced from the second order correction (5.10) of the populations. In contrast to indicators used in other approaches, it is not highly oscillatory.

The momentum adjustment is standardly realized in form of a correction in the direction of the non–adiabatic coupling vector [72]:

$$p_{\mathrm{new}} = \mu(\mu_j \to \lambda, q, p_{\mathrm{old}}) \;=\; p_{\mathrm{old}} \;+\; \tfrac{\alpha}{\|d_{\mu_j\lambda}(q)\|_2}\, d_{\mu_j\lambda}(q),$$

where the scalar coefficient α is chosen such that energy conservation is achieved, i.e., such that

$$\tfrac{1}{2}\left(|p_{\mathrm{new}}|^2 \;-\; |p_{\mathrm{old}}|^2\right) \;=\; \sum\nolimits_\eta |c_\eta^j|^2 E_\eta(q) \;-\; E_\lambda(q).$$

The above version of the scheme can be improved by removing the populations on the energy levels E_λ, $\lambda \neq \mu_j$, of trajectories initially on the μ_jth level when leaving the transition zone, i.e., the region where the indicator Ξ exceeds the threshold Ξ_*. This ensures a Born-Oppenheimer-like motion outside of the transition zone.

Surface hopping algorithms vary mainly in the realization of the hopping procedure. In several aspects, the above proposed QCMD-based variant differs from typical realizations; the interested reader may compare the above algorithmic scheme with the detailed description of typical algorithmic steps in [72] or with the derivation of the standard realization [115].

§4.2 Numerical Example

In this section, the performance of the proposed surface hopping algorithm is presented in application to the avoided crossing example from §2. For comparison, we solved the full Schrödinger equation (2.8) of the problem. Using $N = 2000$ trajectories with randomly distributed initial values sampling the initial wave function, we found an astonishingly good agreement between the purely quantum solution and the result of our surface hopping algorithm. The populations of the wave function components seem to be in accordance to the "exact" solution (cf., Figs. 5.5 and 5.6). But notice, just the absolute value of the components can be obtained by the surface hopping algorithm. The corresponding phase of $\Psi^1_\epsilon(q,t)$ and $\Psi^2_\epsilon(q,t)$ cannot be reconstructed.

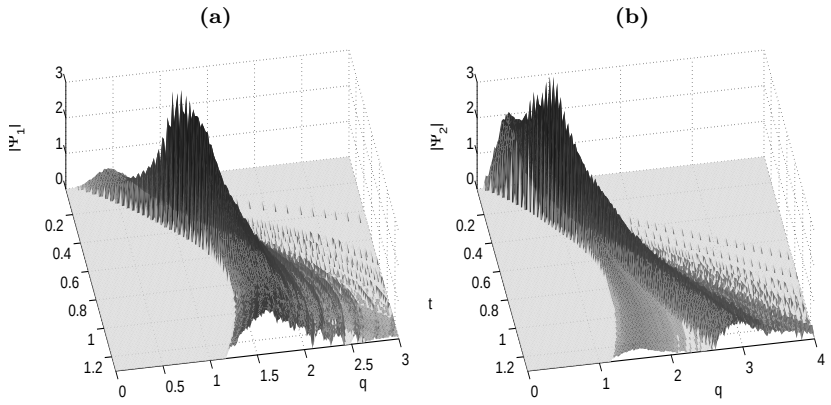

Figure 5.5. QCMD-based surface hopping algorithm: Reconstructed wave packet evolution in q and t . Absolute value of **(a)** Ψ^1_ϵ and **(b)** Ψ^2_ϵ for $\epsilon = 0.01$

Unfortunately, the results of our algorithm strongly depend on the parameters. Obviously, the number of sampling trajectories has a major influence on the accuracy of the computation. The algorithm reacts comparably sensitively on modifications of the transition zone threshold Ξ_* and the size of the time interval Δt. We think that only some careful mathematical analysis of the approximation properties via a novel model analysis — as done in the next section — may be able to cope with these difficulties — which are a common problem of surface hopping methods.

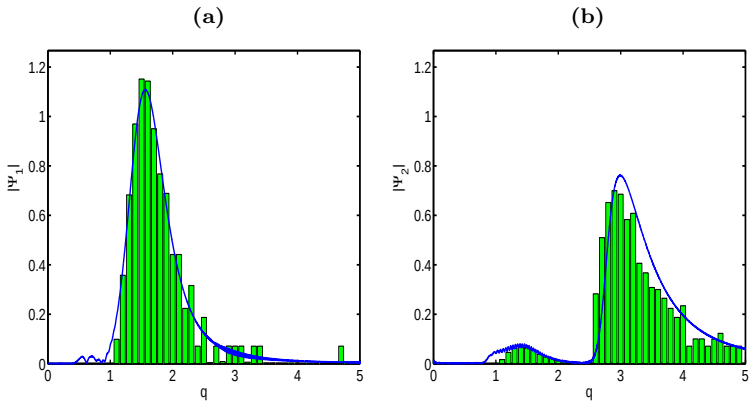

FIGURE 5.6. Comparison of quantum dynamically calculated solution (*lines*) and solution of QCMD-based surface hopping algorithm (*bars*) at time $t = 1.3$. Absolute value of **(a)** $\Psi^1_\epsilon(q, t = 1.3)$ and **(b)** $\Psi^2_\epsilon(q, t = 1.3)$ vs. q for $\epsilon = 0.01$

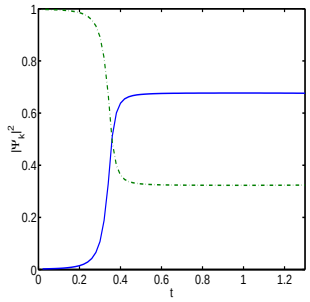

FIGURE 5.7. QCMD-based surface hopping algorithm for $\epsilon = 0.01$: Statistical weights $\|\Psi^1_\epsilon\|_2^2$ (*solid line*) and $\|\Psi^2_\epsilon\|_2^2$ (*dashed dotted*) of the two components of the reconstructed wave function versus t

§5 Quantum–classical Liouville equation

The primary technical tool for the construction of the quantum–classical Liouville equation (QCL) is a *partial Wigner Transform*. It is based on the vector-valued Wigner transform:

Definition 5.3 *For* $\Psi, \Phi \in L^2(\mathbb{R}^d)^N$ *the* Wigner matrix *is defined by*

$$W_\epsilon(\Psi, \Phi)(q, p) \;=\; (2\pi)^{-d} \int_{R^d} \Psi\left(q - \epsilon\frac{y}{2}\right) \otimes \Phi^*\left(q + \epsilon\frac{y}{2}\right) \exp(ip^T y)\, dy, \tag{5.11}$$

where $\otimes$ *defines the tensor product of vectors.*

Remark. The *Wigner transform* [118] itself and its asymptotic properties were thoroughly studied by Gérard, Markowich et al. [34]. It received considerable attention due to its ability to reformulate quantum dynamical expectation values in terms of their classical counterparts.

Remark. Obviously, the Wigner transform of Definition 5.3 is applied to the q–coordinate only, leaving the "quantum nature" in the other degree of freedom untouched.

Instead of transforming now the solution of the full quantum system (5.1), we focus on the Schrödinger equation in the adiabatic basis (5.5). Therefore, we reformulate our system with respect to the expansion coefficients $c_\epsilon = c_\epsilon(q,t) = (c_\epsilon^\lambda(q,t))$.

Definition 5.4 *The* Wigner density matrix *corresponding to the Schrödinger equation in an adiabatic basis (5.5) is*

$$\mathcal{W}_\epsilon(q,p,t) \;=\; W_\epsilon(c_\epsilon(\cdot,t), c_\epsilon(\cdot,t))(q,p). \tag{5.12}$$

with initial value $\mathcal{W}_*(q,p,t) \;=\; W_\epsilon(c_*(\cdot), c_*(\cdot))(q,p)$.

Note that this Wigner density matrix $\mathcal{W}_\epsilon$ is a Hermitian matrix. The equations of motion for $\mathcal{W}_*(q,p,t)$ are given in [103]. However, the cost of solving these equations exceeds by far the cost of solving the original Schrödinger equation (5.1) since one has to deal with a PDE of N^2 degrees of freedom now.

Therefore, consider the following approximation to the equations of motion of $\mathcal{W}_\epsilon$ with the advantage of various "cheap" approaches to a solution:

Definition 5.5 *The equation*

$$\begin{aligned} \partial_t\, \rho_\epsilon^{\mathrm{ad}}(q,p,t) \quad &= \quad -\tfrac{i}{\epsilon}\left[\, E(q) - i\epsilon p\cdot \mathcal{C}(q)\,,\, \rho_\epsilon^{\mathrm{ad}}(q,p,t)\right]_- \\ &\quad\; -p\cdot D_q \rho_\epsilon^{\mathrm{ad}}(q,p,t) \;+\; \tfrac{1}{2}\left[D_q E(q), D_p \rho_\epsilon^{\mathrm{ad}}(q,p,t)\right]_+ . \end{aligned} \tag{5.13}$$

with initial conditions $\rho_\epsilon^{\mathrm{ad}}(t=t_0) = W^\epsilon(c_*,c_*)$ *given by the initial conditions* $c_* = c_\epsilon(t=t_0)$ *of the Schrödinger equation (5.5), is called the* adiabatic version *of the* quantum-classical Liouville equation (QCL)*; we refer to its solution* $\rho_\epsilon^{\mathrm{ad}} = \rho_\epsilon^{\mathrm{ad}}(q,p,t)$ *as to the* adiabatic QCL solution*. Note that* $[\cdot,\cdot]_\pm$ *denotes the usual commutator and anti-commutator, i.e.,* $[A,B]_\pm = AB \pm BA$ *for two square matrices* A, B*.*

A rigorous mathematical analysis justifies the quantum-classical Liouville equation and proves the validity of solution $\rho_\epsilon^{\mathrm{ad}}$ with respect to the original solution $\mathcal{W}_\epsilon$ Since the following statements result from studying the asymptotic expansion of the action of some pseudo-differential operator under the Wigner transform, we have to make following assumptions:

(PD1) Suppose that[2]

$$\mathcal{H}^S(q,p) \;=\; \tfrac{1}{2}|p|^2 \;+\; E(q) \;+\; \tfrac{1}{2}T(q) - \;i\epsilon\, \mathcal{C}(q)\cdot p \;+\; \frac{\epsilon^2}{2} D_q\cdot \mathcal{C}(q)$$

is a uniformly smooth matrix-valued symbol for all $0 < \epsilon < \epsilon_0$, i.e., $\mathcal{H}^S \in C^\infty(\mathbb{R}^d \times \mathbb{R}^d)^{n\times n}$ such that, for some $M \geq 0$ and every multi-index $\alpha \in \mathbb{N}^d \times \mathbb{N}^d$,

$$|D^\alpha_{(q,p)} \mathcal{H}^S(q,p)| \;\leq\; C_\alpha (1+|p|)^M,$$

component wise.

[2] $D_q \cdot \mathcal{C}$ denotes a matrix with entries $(D_q\cdot\mathcal{C})_{kl} = \sum_j D_{q_j}\mathcal{C}^j_{kl}$

(PD2) Let the operator

$$E - \frac{\epsilon^2}{2}\Delta_q + \frac{\epsilon^2}{2}T - \epsilon^2\,\mathcal{C}\cdot D_q$$

be essentially self-adjoint on $L^2(\mathbb{R}^d)^N$.

Theorem 5.6 (Thm. 4.2 and Thm. 4.5 of [103]) *Let the assumptions (E4), (PD1) and (PD2) be valid and $\epsilon > 0$. Let $c_\epsilon = c_\epsilon(q,t)$ be the solution of (5.5) with (uniformly) normalized initial conditions $c_* = c_\epsilon(t = t_0)$.*[3] *Moreover, let $W_\epsilon(c_\epsilon, c_\epsilon)$ denote the corresponding partial Wigner transform. Further, let the solution of the adiabatic QCL (5.13) with initial condition $\rho_\epsilon^{\mathrm{ad}}(\cdot,\cdot,t_0) = W_\epsilon(c_*, c_*)$ be given. Then, the solution of the adiabatic QCL is an $\mathcal{O}(\epsilon)$ approximation for finite time spans $t \in [t_0, T]$:*

$$\rho_\epsilon^{\mathrm{ad}} = W_\epsilon(c_\epsilon, c_\epsilon) + \mathcal{O}(\epsilon)$$

in a suitable space (for details, see [103]).

Furthermore, for any sufficiently rapid decreasing observable A there exists some constant C such that for all $\epsilon > 0$ and for all $t \in [0,T]$:

$$|\langle W_\epsilon(c_\epsilon, c_\epsilon), A\rangle - \langle \rho^\epsilon, A\rangle| < C\,\epsilon \tag{5.14}$$

with

$$\langle \rho, A\rangle = \int_{\mathbb{R}^d}\int_{\mathbb{R}^d} tr(\rho A^*)\,dp\,dq.$$

Remark.

- A generalized version of the definition of QCL as well as of Thm. 5.6 can be found in [103].
- Analogously one can construct a diabatic version of QCL based on (5.1)

$$\begin{aligned}\partial_t\,\rho_\epsilon^{\mathrm{d}}(q,p,t) &= -\tfrac{i}{\epsilon}\left[H(q)\,,\,\rho_\epsilon^{\mathrm{d}}(q,p,t)\right]_- \\ &\quad - p\cdot D_q\rho_\epsilon^{\mathrm{d}}(q,p,t) + \tfrac{1}{2}\left[D_qH(q), D_p\rho_\epsilon^{\mathrm{d}}(q,p,t)\right]_+ .\end{aligned} \tag{5.15}$$

  In this case, Thm. 5.6 is even valid without assumption (E4).
- The next terms in the expansion can also be computed on the basis of [57, Sec. 18.5].
- For the solution of the adiabatic QCL (5.13), note that the RHS includes a "quantum" propagation on the modified energy levels $E(q) - i\epsilon p\cdot\mathcal{C}(q)$ plus a kind of "classical" dynamics on the energy level $E(q)$ corresponding to the Liouville equation. This gives the opportunity to construct methods quite similar to surface hopping methods: a classical Born–Oppenheimer dynamics (cf., the lower right branch of Fig. 5.8) coupled to stochastically modeled transitions in the populations.

[3] That is, for all values of ϵ, the family of initial conditions is lying on the unit sphere in $L^2(\mathbb{R}^d)^N$

- In comparison, the RHS of the diabatic QCL (5.15) can be represented by a deterministic QCMD–like dynamics combined with a stochastic sampling of the density (see the lower left branch of Fig. 5.8).

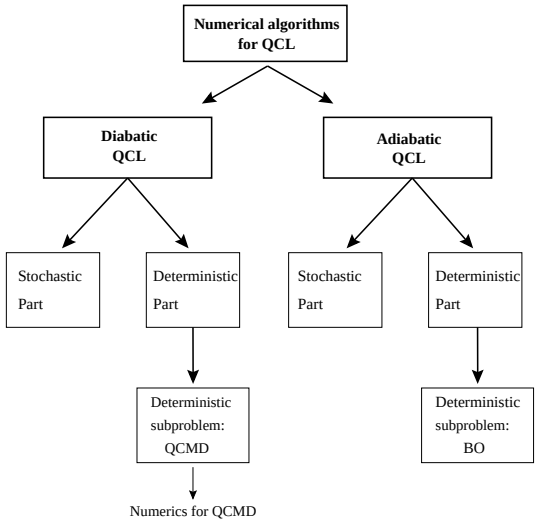

Figure 5.8. The particular structure of the QCL equations suggests a representation in a stochastic as well as deterministic subproblem. For the diabatic QCL, the deterministic subproblem is QCMD–like.